

Technical Note

High Chlorophyll-a Areas along the Western Coast of South Sulawesi-Indonesia during the Rainy Season Revealed by Satellite Data

Anindya Wirasatriya ^{1,2,*}, Raden Dwi Susanto ^{3,4}, Joga Dharma Setiawan ^{2,5}, Fatwa Ramdani ^{6,7}, Iskhaq Iskandar ⁸, Abd. Rasyid Jalil ⁹, Ardiansyah Desmont Puryajati ^{1,10}, Kunarso Kunarso ¹ and Lilik Maslukah ¹

- ¹ Department of Oceanography, Faculty of Fisheries and Marine Sciences, Diponegoro University, Semarang 50275, Indonesia; desmont213@alumni.undip.ac.id (A.D.P.); kunarso@lecturer.undip.ac.id (K.K.); lilikmaslukah@lecturer.undip.ac.id (L.M.)
 - ² Center for Coastal Disaster Mitigation and Rehabilitation Studies, Diponegoro University, Semarang 50275, Indonesia; joga.setiawan@ft.undip.ac.id
 - ³ Department of Atmospheric and Oceanic Science, University of Maryland, College Park, MD 20742, USA; dwisusa@umd.edu
 - ⁴ Faculty of Earth Science and Technology, Bandung Institute of Technology, Bandung 40132, Indonesia
 - ⁵ Department of Mechanical Engineering, Faculty of Engineering, Diponegoro University, Semarang 50275, Indonesia
 - ⁶ Geoinformatics Research Group, Faculty of Computer Science, Brawijaya University, Malang 65145, Indonesia; fatwaramdani@ub.ac.id
 - ⁷ Graduate School of Humanities and Social Sciences, University of Tsukuba, Tsukuba 305-8571, Japan
 - ⁸ Department of Physics, Faculty of Mathematics and Natural Sciences, Sriwijaya University, Indralaya 30662, Indonesia; iskhaq@mipa.unsri.ac.id
 - ⁹ Faculty of Marine Science and Fisheries, Departement of Marine Science, Hasanuddin University, Makassar 90245, Indonesia; abdrasyid@unhas.ac.id
 - ¹⁰ Algmarine, Department of Oceanography, Diponegoro University, Semarang 50275, Indonesia
- * Correspondence: anindyawirasatriya@lecturer.undip.ac.id; Tel.: +62-247474698

Citation: Wirasatriya, A.; Susanto, R.D.; Setiawan, J.D.; Ramdani, F.; Iskandar, I.; Jalil, R.; Puryajati, A.D.; Kunarso, K.; Maslukah, L. High Chlorophyll-a Areas along the Western Coast of South Sulawesi-Indonesia during the Rainy Season Revealed by Satellite Data. *Remote Sens.* **2021**, *13*, 4833. <https://doi.org/10.3390/rs13234833>

Academic Editor: Ali Khenchaf

Received: 26 September 2021

Accepted: 25 November 2021

Published: 28 November 2021

Publisher's Note: MDPI stays neutral with regard to jurisdictional claims in published maps and institutional affiliations.



Copyright: © 2021 by the authors. Licensee MDPI, Basel, Switzerland. This article is an open access article distributed under the terms and conditions of the Creative Commons Attribution (CC BY) license (<https://creativecommons.org/licenses/by/4.0/>).

Abstract: The southern coast of South Sulawesi-Indonesia is known as an upwelling area occurring during dry season, which peaks in August. This upwelling area is indicated by high chlorophyll-a (Chl-a) concentrations due to a strong easterly wind-induced upwelling. However, the investigation of Chl-a variability is less studied along the western coast of South Sulawesi. By taking advantages of remote sensing data of Chl-a, sea surface temperature, surface wind, and precipitation, the present study firstly shows that along the western coast of South Sulawesi, there are two areas, which have high primary productivity occurring during the rainy season. The first area is at 119.0° E–119.5° E; 3.5° S–4.0° S, while the second area is at 119.0° E–119.5° E; 3.5° S–4.0° S. The maximum primary productivity in the first (second) area occurs in April (January). The generating mechanism of the high primary productivity along the western coast of South Sulawesi is different from its southern coast. The presence of river runoff in these two areas may bring anthropogenic organic compounds during the peak of rainy season, resulting in increased Chl-a concentration.

Keywords: primary productivity; chlorophyll-a; precipitation; sea surface temperature; South Sulawesi-Indonesia

1. Introduction

Chlorophyll-a (Chl-a) is an indicator for phytoplankton biomass, which becomes the most important driver of ocean ecosystem health and productivity. As the first trophic level, phytoplankton biomass transfers both material and energy to higher-trophic-level organisms. Thus, as a connection of food chain sequence, Chl-a concentration determines the biomass of fish and therefore, regulates the fish catch production in an area. The

higher Chl-a concentration corresponds to the higher catch of fishes. Welliken et al. [1] reported a strong positive correlation between the catch of mackerel fish and Chl-a concentration in the Arafura Sea. Furthermore, Welliken et al. [2] also reported that the variation of skipjack tuna catches is influenced by Chl-a concentration in the Savu Sea. During August and September, the peak of Chl-a concentration becomes the potential fishing season for skipjack tuna in the Savu Sea. For the southern coast of Java, Lahlali et al. [3] found that the catch per unit effort of tuna fish increases along with the increase of Chl-a concentration and the decrease of sea surface temperature (SST). Thus, understanding the characteristics of Chl-a variability in an area is a key success for fishery management.

To date, the big picture of the variability of Chl-a in the Indonesian Maritime Continent (IMC) has been investigated by Siswanto et al. [4]. Using more than two decades of data of the satellite-based Chl-a, they managed to reveal the distinct spatio-temporal distribution of Chl-a associated with different climate events. In the coastal area of IMC, Chl-a mostly varies by the fluctuation of rainfall/river discharge. Meanwhile, in the open ocean, the mechanisms of the wind generated upwelling and downwelling dominantly controls the variability of Chl-a in the IMC.

As part of the IMC, the sea of South Sulawesi was less emphasized in the study of Siswanto et al. [4]. The sea off the southern coast of South Sulawesi is a well-known high Chl-a area during the peak of the boreal summer (gray box in Figure 1) [5,6]. By analyzing satellite data, Setiawan and Kawamura [5] found that the strong easterly wind blowing during the boreal summer monsoon corresponds to the events of Chl-a blooming and SST cooling at the southern coast of South Sulawesi. Furthermore, the evidence of the upwelling event was found by Utama et al. [6] by using a combination of Conductivity Temperature Depth (CTD) observation and reanalysis data. As indicated by their CTD data, the elevated cooler water mass proves the upwelling occurrence near the southern coast of South Sulawesi. They suggested that the offshore Ekman transport of around $8.5 \text{ m}^2/\text{s}$ causes this upwelling.

The topography of South Sulawesi is complex, as seen in Figure 1. The southern (red box) and northern (blue box) parts of the south of Sulawesi are separated by two mountain ranges. The bathymetry of the sea off the western coast of South Sulawesi is deeper in the north than in the south. Nurdin et al. [7] investigated the variability of Chl-a along the western coast of South Sulawesi. However, their research was limited to the Spermonde Islands (black box at Figure 1). They discovered that the Chl-a at the Spermonde Islands during the summer season is higher than during the rainy season. Furthermore, the Chl-a variation at the Spermonde Islands corresponds to the fishing ground of *Rastrelliger kanagurta* [8]. Therefore, the whole area along the western coast of the South Sulawesi has never before been explored.

In the present study, we investigate the variability of Chl-a for the whole area along the western coast of South Sulawesi. In Section 2 we explain the merging product of satellite-based Chl-a data as a proxy of primary productivity to reach the maximum coverage of the Chl-a, an observation that was used in this study. In addition, SST, surface wind, and rainfall data were also used for investigating its underlying mechanisms. The results and discussion are presented in Section 3, which emphasizes the spatial and temporal variation of Chl-a, surface wind, and precipitation in the study area. Finally, the conclusion is presented in Section 4.

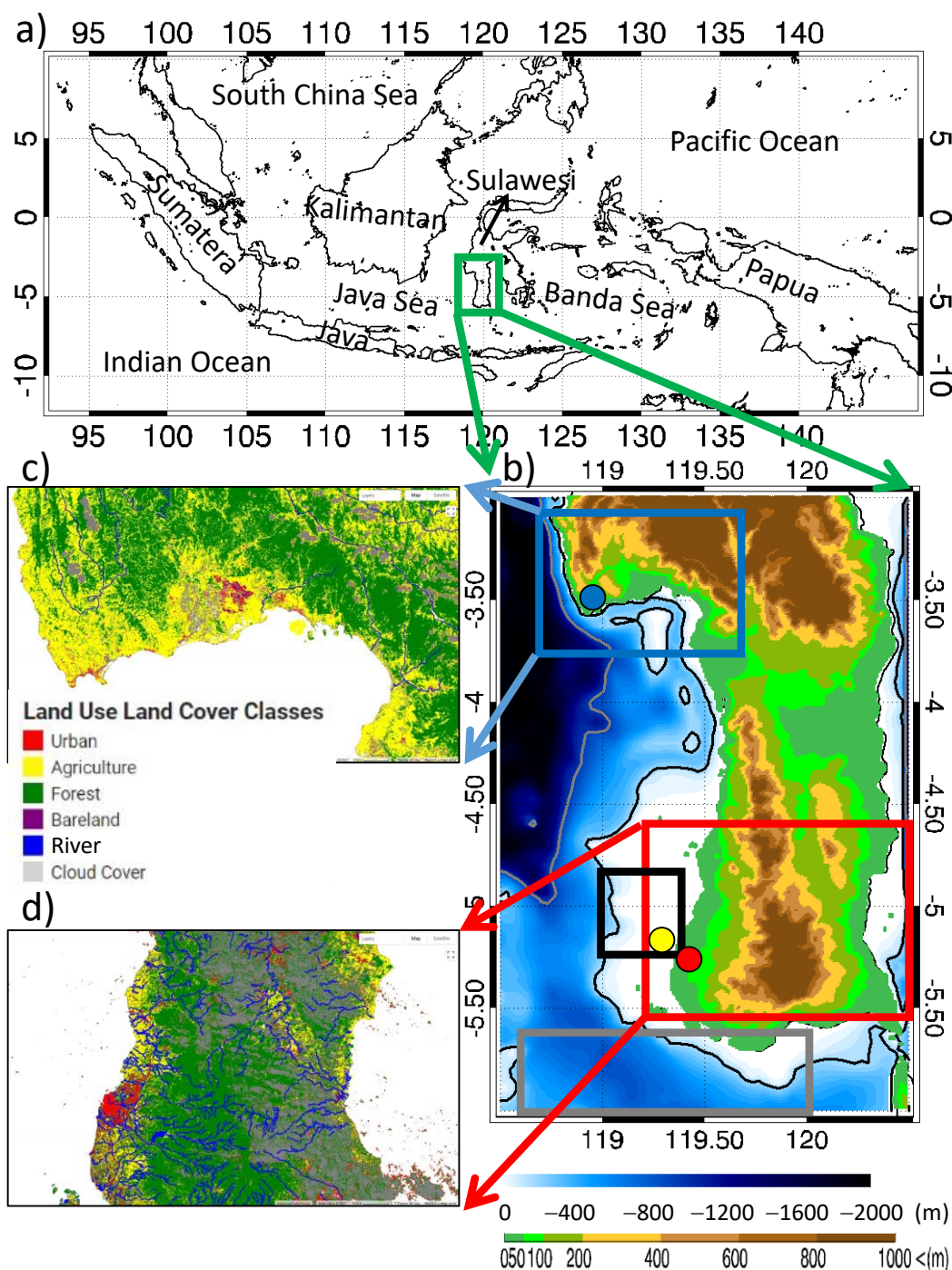


Figure 1. (a) Indonesian seas. (b) Bathymetry and topography of the South Sulawesi. The black and gray contours denote isobaths of 200 m and 1000 m, respectively. The gray box represents the well-known upwelling area that occurs during boreal summer, as reported by Setiawan and Kawamura [5]. The black box denotes the location of the Spermonde Islands. The blue and red dots denote the meteorological stations at Majene Regency and Makassar City, respectively. The yellow dot denotes the location of Barrang Caddi Island where in situ data collection was conducted on 8 September 2020. The blue (c) and red (d) boxes denote the area with mountainous ranges at the northern and southern part of the South Sulawesi, respectively. The land cover of (c,d) are obtained from Landsat 8 images on 15 March 2020 and 3 June 2020, respectively.

2. Dataset and Methods

2.1. Data

We used blended multi satellites Chl-a products from the Ocean Color-Climate Change Initiative version 4.2 (OC-CCI 4.2) to investigate the primary productivity along

the western coast of the South Sulawesi [9]. These data have daily and 4 km temporal and spatial resolutions, respectively. The Chl-a measurements from the Medium Resolution Imaging Spectrometer (MERIS), Aqua-Moderate Resolution Imaging Spectroradiometer (MODIS), Sea-Viewing Wide Field-of-View Sensor (SeaWiFS), and the Visible Infrared Imaging Radiometer Suite (VIIRS) were used for OC-CCI data production. Remote sensing reflectant (Rrs) 443, Rrs 555, phytoplankton absorption coefficient at 443 nm (aph 443), and particulate backscattering coefficient for dissolved and detrital material at 555 nm (bbp 555) of OC-CCI 4.2 were also used for examining the suspended sediment contamination in the observed Chl-a concentration. Rrs 443 (Rrs 555) estimates the existence of phytoplankton (suspended sediment) due to the strong absorption (reflectant) of Rrs 443 by phytoplankton (Rrs 555 by suspended sediment) [10,11]. Thus, the higher aph 443 and bbp 555 denote the more phytoplankton biomass and higher suspended sediment concentration.

SST data was from the daily group for the High-Resolution Sea Surface Temperature (GHRSSST) Level 4 Multiscale Ultrahigh Resolution (MUR) analysis with the spatial resolution of 0.01° [12,13]. This dataset is based upon nighttime GHRSSST L2P skin and subskin SST observations from several instruments, including the NASA Advanced Microwave Scanning Radiometer-EOS (AMSR-E), the JAXA Advanced Microwave Scanning Radiometer 2 on GCOM-W1, the Moderate Resolution Imaging Spectroradiometers (MODIS) on the NASA Aqua and Terra platforms, the US Navy microwave WindSat radiometer, the Advanced Very High Resolution Radiometer (AVHRR) on several NOAA satellites, and in situ SST observations from the NOAA iQuam project. This SST product has been evaluated against the in situ observations [14].

A semi-daily Advanced Scatterometer (ASCAT) with a spatial resolution of $0.125^\circ \times 0.125^\circ$ was used for investigating the surface wind variation [15]. Furthermore, we used an hourly precipitation product from Global Satellite Mapping for Precipitation (GSMaP) with a spatial resolution of $0.1^\circ \times 0.1^\circ$ [16]. GSMaP product was constructed from the Dual-frequency Precipitation Radar (DPR) onboard GPM core satellites, other GPM constellation satellites, and Geostationary satellites. In the present study, our analysis was based on the original spatial resolution of each dataset without any interpolation. In addition, we also analyzed the precipitation data obtained from meteorological stations at Makassar City and Majene Regency, as shown in Figure 1b.

On 8 September 2020, we conducted field observation in the sea around Barrang Caddi Island, which is part of the Spermonde Islands (Figure 1). We took water samples from 26 stations and analyzed the Chl-a concentration and total suspended sediment (TSS). The detail methods of the field sampling and analysis can be found in Maslukah et al. [17].

2.2. Method

The method of this study was based on the climatological analysis from 13 years of data (2007–2019) of each variable. Firstly, hourly and semi-daily data were composited into daily data. Then, all daily data were composited into monthly and monthly climatology following Wirasatriya et al. [18],

$$\bar{X}(x, y) = \frac{1}{n} \sum_{i=1}^n x_i(x, y, t) \quad (1)$$

where $\bar{X}(x, y)$ is the monthly mean value or monthly climatology value at position (x, y) , $x_i(x, y, t)$ is i -th value of the data at (x, y) position and time t . Next, n is the number of days in a one month period and the number of months in one period of climatology for the monthly calculation and monthly climatology calculation, respectively. Furthermore, x_i is excluded in the calculation if that pixel is hollow.

3. Results

3.1. Spatial Distribution of Chl-a, SST, and Surface Wind

First, we present the spatial distribution of Chl-a, SST, and surface wind along the western coast of South Sulawesi in August (Figure 2). The high Chl-a concentration appears in two areas. The first area is at 119.0° E– 119.5° E; 3.5° S– 4.0° S. In this area the high Chl-a concentration corresponds to the low SST and strong easterly wind. This strong easterly wind comes from the gap between the mountain ranges known as the expansion fan. The mechanisms of the strong wind off the wind gap are possibly due to the drop of the marine atmospheric boundary layer height after passing the gap, which accelerates the wind speed (e.g., [19,20]). The expansion fan phenomenon is also detected at the gap between the Gorontalo Mountain and the Sulawesi Mountain, described by Wirasatriya et al. [21]. Since the first area is located in the southern hemisphere, the strong easterly wind may generate southward offshore Ekman transport that causes coastal upwelling, reducing SST and enhancing Chl-a concentration. This offshore Ekman transport mechanism is also found in the coastal upwelling event along the southern coast of Java during the summer monsoon [22]. However, the magnitudes of enhancing Chl-a and reducing SST are less than those at the southern coast of the South Sulawesi, as described by Setiawan and Kawamura [5] and Utama et al. [6]. The second area is the Spermonde Islands, which are located at 119.0° E– 119.5° E; 4.6° S– 5.1° S. Unlike the first area, the enhancing Chl-a concentration at the second area in January does not relate to SST and surface wind speed (Figure 3). The high Chl-a in the second area occurs under the weak wind and warm SST conditions. This may indicate that other factors, rather than wind speed, are influencing the high Chl-a concentration in the Spermonde Islands.

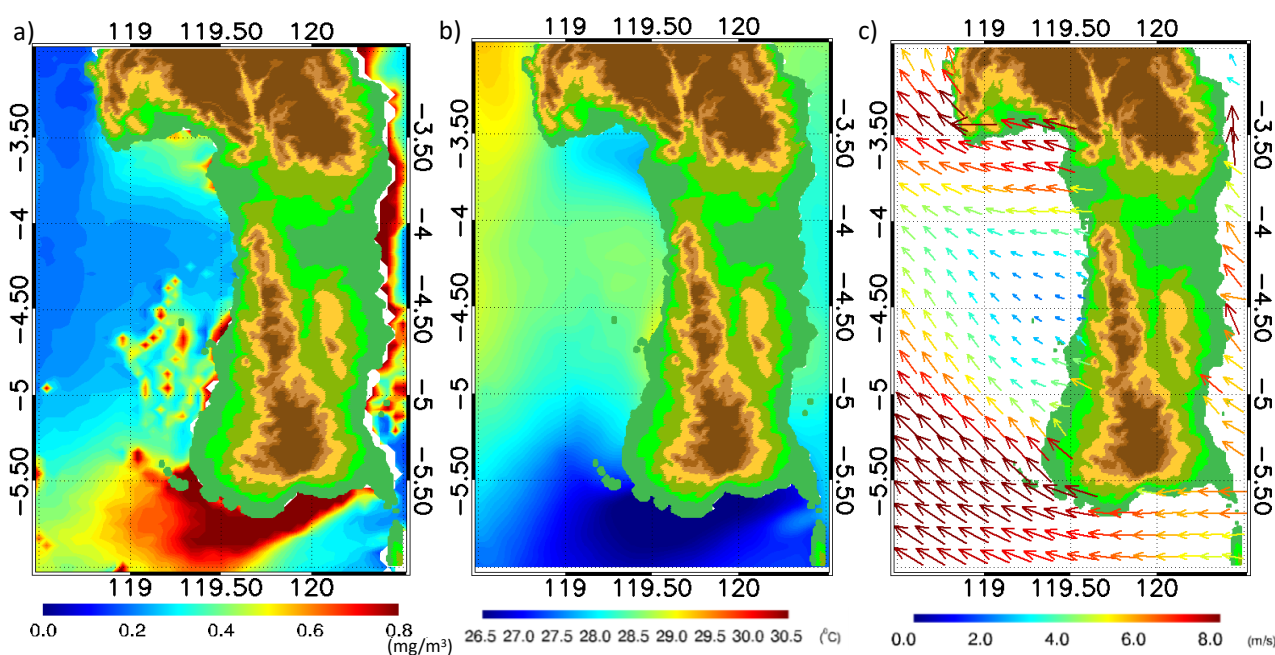


Figure 2. Spatial distribution of (a) Chl-a, (b) SST, and (c) surface wind along the western coast of South Sulawesi in August climatology (2007–2019).

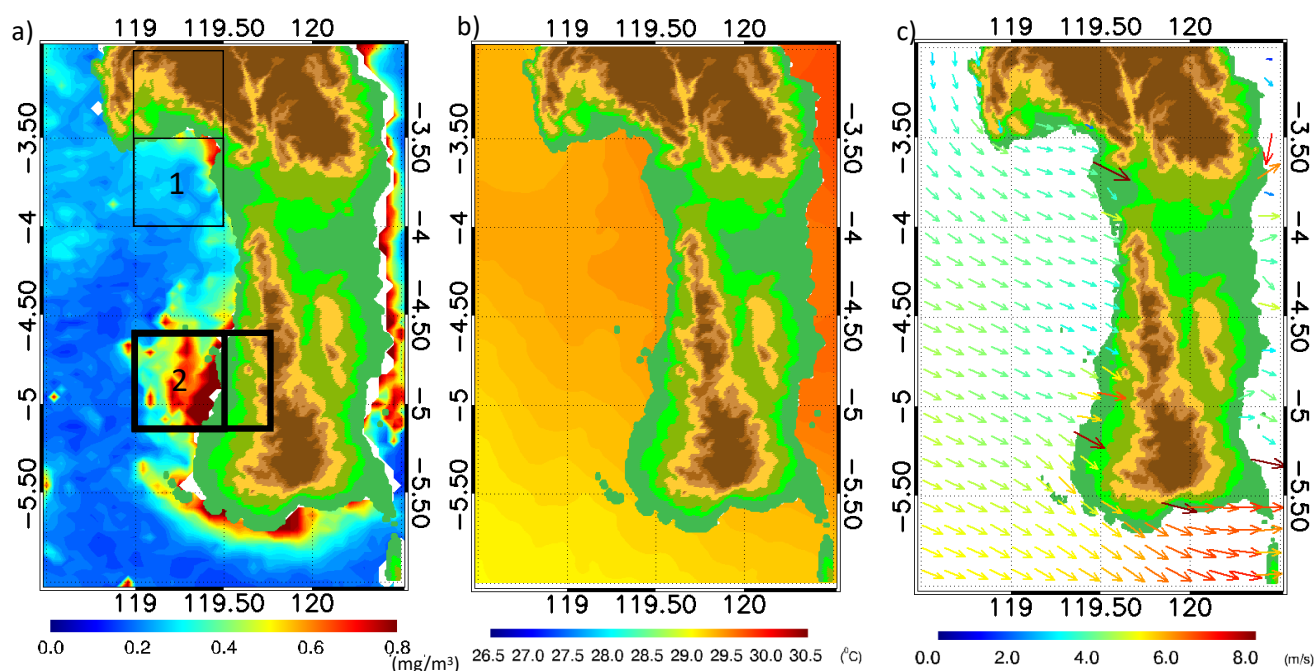


Figure 3. Spatial distribution of (a) Chl-a, (b) SST, and (c) surface wind along the western coast of South Sulawesi in January climatology (2007–2019). The boxes denote the sampling area for temporal analysis shown in Figure 4. Thin box represents the high Chl-a area in the northern part of the western coast of South Sulawesi and becomes the first focused area of analysis, while the thick box is for the southern part and becomes a second focused area of analysis. The averaged areas for precipitation in the boxes are extended to the land to investigate the river runoff influence on the variability of Chl-a along the western coast of the South Sulawesi.

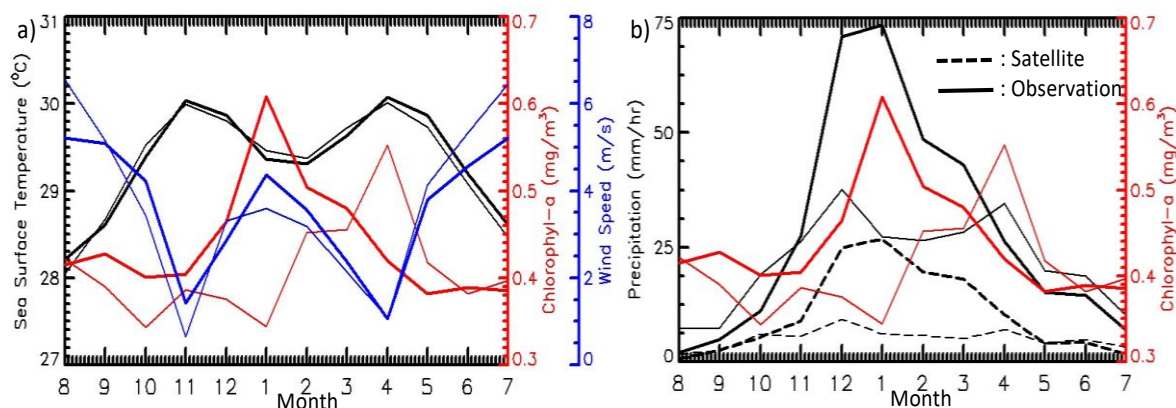


Figure 4. Temporal variation of (a) SST, Chl-a, and wind speed; and (b) precipitation and Chl-a. Thin and thick lines represent the thin and thick boxes in Figure 3a. The observational data of precipitation are derived from meteorological stations at Majene Regency (blue dot) and Makassar City (red dot), as shown in Figure 1b. For precipitation derived from satellite, the averaging area includes the land area, as shown by the extension of boxes in Figure 3a.

3.2. Temporal Analysis of Chl-a, SST, Surface Wind, and Precipitation

Temporal variability of SST, Chl-a, and wind speed are shown in Figure 4a. It is clearly shown that the variabilities of SSTs in both areas follow the variabilities of wind speed. The higher the wind speed, the lower SST will be, and vice versa. In contrast, the variabilities of Chl-a in both areas are almost independent of the variabilities of wind speed. There are two Chl-a peaks in the first area (thin box), which occur in August and April. Chl-a concentrations reach 0.41 mg/m^3 in August. This is related to the high wind speed of roughly 6.5 m/s that promotes coastal upwelling, as discussed in the previous section. In April, the concentration of Chl-a reaches its maximum (i.e., 0.55 mg/m^3), but this occurs under the condition of minimum wind speed (i.e., 1 m/s).

Chl-a concentrations in the second area (thick line) are generally higher than those in the first area throughout the whole year, except for April, the first area's peak. The whole monthly climatology of Chl-a is higher than 0.39 mg/m^3 . An outstanding maximum Chl-a concentration occurs in January when Chl-a concentration reaches 0.6 mg/m^3 . However, the variability of Chl-a concentration in the second area is not consistent with the variability of wind speed. Although intense wind speed in January may contribute to the increase of Chl-a concentration, August's most vigorous wind speed does not result in the highest Chl-a. Therefore, another factor controls the occurrence of the highest Chl-a concentration in the first (second) area in April (January).

To address the incongruity of the relationship between wind speed and Chl-a, we plot the temporal variability of precipitation and Chl-a in both areas in Figure 4b. We extend the average precipitation area to the upland area to account for the potential impact of the river runoff during the rainy season. We also plot the precipitation observed from meteorological stations at Majene Regency and Makassar City, which represent the first and second areas, respectively. The variability of precipitation derived from satellites have similar pattern with the observed precipitations. The amplitude difference during the peak of precipitation may be due to the areal representative differences of both data. The peak of Chl-a concentration in January at the second area and in April at the first area corresponds to precipitation. Thus, the variability of the Chl-a concentration in both areas is more strongly influenced by precipitation. This finding is supported by the correlation analysis presented in Table 1. SST versus wind speed has strong negative correlations in both areas, indicating that SST is highly dependent on wind speed. The correlation coefficient between Chl-a and wind speed, on the other hand, is minimal, which is ≤ 0.4 . The higher correlations are shown by Chl-a versus precipitation i.e., 0.43 and 0.51 for the first and second areas, respectively. This means that the precipitation has a greater impact on Chl-a variation than wind speed. The terrestrial nutrient input brought by river runoff during the rainy season may be the mechanism by which precipitation influences Chl-a variation. As shown by Maslukah et al. [23], the phosphate influx in the northern shore of Java is driven by river runoffs that transport organic materials. However, combining the independent variables of wind speed and precipitation may have a greater impact on Chl-a variability than each variable alone. The correlation coefficients for the first and second areas increased to 0.46 and 0.58, respectively. This finding could explain how wind speed affects Chl-a regulation during the boreal summer monsoon.

Table 1. Significant correlation analysis ($p < 0.05$) among SST, Chl-a, wind speed, and precipitation from satellite.

Variable	SST		Chl-a	
	First Area	Second Area	First Area	Second Area
Wind speed	-0.79	-0.73	0.35	0.40
Precipitation			0.43	0.51
Wind speed and precipitation			0.46	0.58

3.3. Possibility of Suspended Sediment That Bias the Observed Chl-a Concentration

The nutrient influx from river runoff may come along with the organic sediment particles, increasing the turbidity in the coastal seas, then possibly turning the study area into case-2 waters. The NASA OC4v4 standard algorithm, on the other hand, was used to extract the standard Chl-a product, which is only suited for case-1 waters and may fail to recover Chl-a consistently in case-2 waters [24]. This section examined the presence of suspended sediment that could influence the Chl-a value in the western coast of South Sulawesi by using Rrs 443 and 555 (Figure 5). This method has also been used by Wirasatriya et al. [25] for examining the potential contamination of satellite Chl-a measurements by suspended sediment within the Indonesian sea. Low Rrs 443 appears in the first and second areas, corresponding to phytoplankton biomass's existence in both areas. However, low Rrs 555 is only detected in the first area. This means that the observed Chl-a

concentration in the first area is not contaminated by suspended sediment. In contrast, high Chl-a concentration in the second area is co-located with the high Rrs 555. Furthermore, the area with low Rrs 443 (high Rrs 555) corresponds to the area with high aph 443 (high bbp 555), which denotes the high phytoplankton absorption coefficient at 443 nm, and the high particulate backscattering coefficient, at 555 nm. Thus, the observed Chl-a in the second area may be biased by the condition of turbid water. A further explanation is depicted in the scatter plots shown in Figure 6. For the relation between Rrs 443 and Chl-a, both areas show the same tendency i.e., the lower Rrs 443, the higher Chl-a (Figure 6a,c). However, this relation is more scattered in the second area, indicating the stronger bias in the second area than the first area. In the first area, the Rrs 555 is low, distributed from $1.2 \times 10^{-3} \text{ sr}^{-1}$ – $3.2 \times 10^{-3} \text{ sr}^{-1}$. This explains the low suspended sediment in the first area. In contrast, the high Rrs 555 in the second area, distributed from $2 \times 10^{-3} \text{ sr}^{-1}$ – $4.5 \times 10^{-3} \text{ sr}^{-1}$ (Figure 6b,d) indicates the existence of high suspended sediments, which may bias the Chl-a measurement. This result is supported with an in situ observation, as shown in Figure 7. Although the correlation is weak and the coefficient of determination is low, we still can see the linear trend, which shows the higher the Chl-a, the higher the TSS concentration. The weak correlation between in situ Chl-a and in situ TSS is common in the coastal waters, as also shown by Maslukah et al. [26], probably due to the limitation of the data population. We also cannot obtain the correlation between the Chl-a satellite and in situ Chl-a, due to the cloudy condition during field observation. Thus, the high Chl-a observed in the second area is contaminated by the high-suspended sediment. Further investigation is needed to obtain the typical algorithm for estimating Chl-a in the second area, which is classified as case-2 water. This task is left for future study.

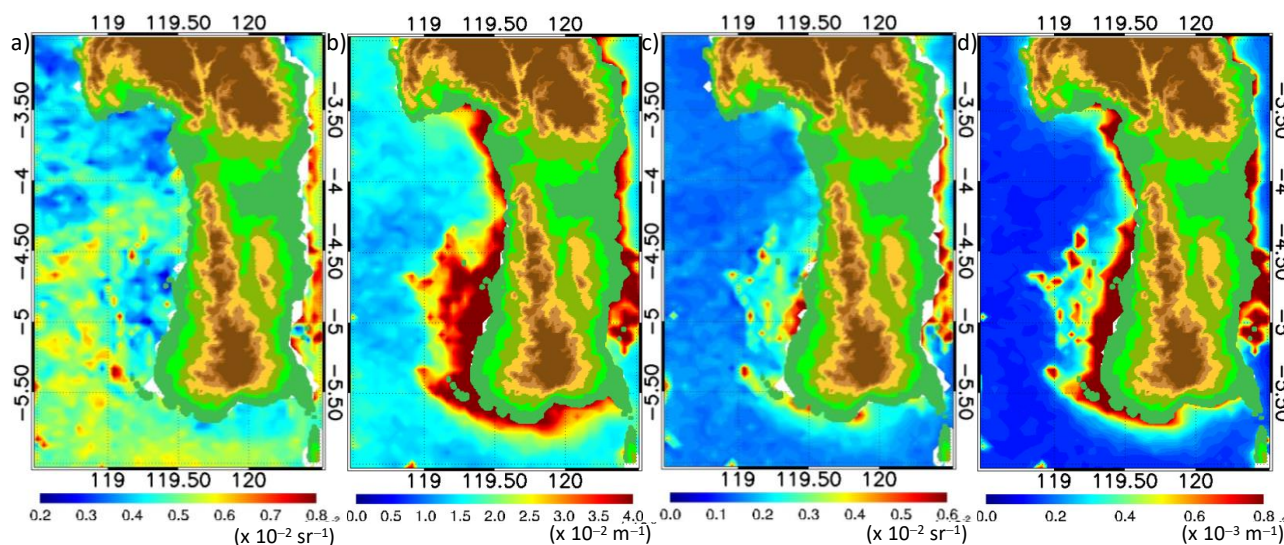


Figure 5. The spatial distribution of (a) Rrs 443, (b) aph 443, (c) Rrs 555, and (d) bbp 555 along the western coast of South Sulawesi in January climatology (2007–2019). Lower Rrs 443 and higher aph 443 denote the existence of phytoplankton, while higher Rrs 555 and higher bbp 555 denote the existence of suspended sediment.

As shown earlier, the suspended sediment in the first area is lower than that in the second area. This could be because the first area receives less precipitation than the second. Furthermore, as shown in Figure 1, the difference in land cover between areas may contribute to the varying sediment influx between the two areas. The upland side of the second area has more rivers than the first, which pass through the agricultural and urban areas. The sediment influx from the upland area brought by the river runoff during the rainy season that passes through the agriculture and urban areas is responsible for the high-suspended sediment at the high Chl-a areas. Therefore, it may suggest that the anthropogenic activities in the upland area determine the organic sediment matter that influences Chl-a concentration in both areas.

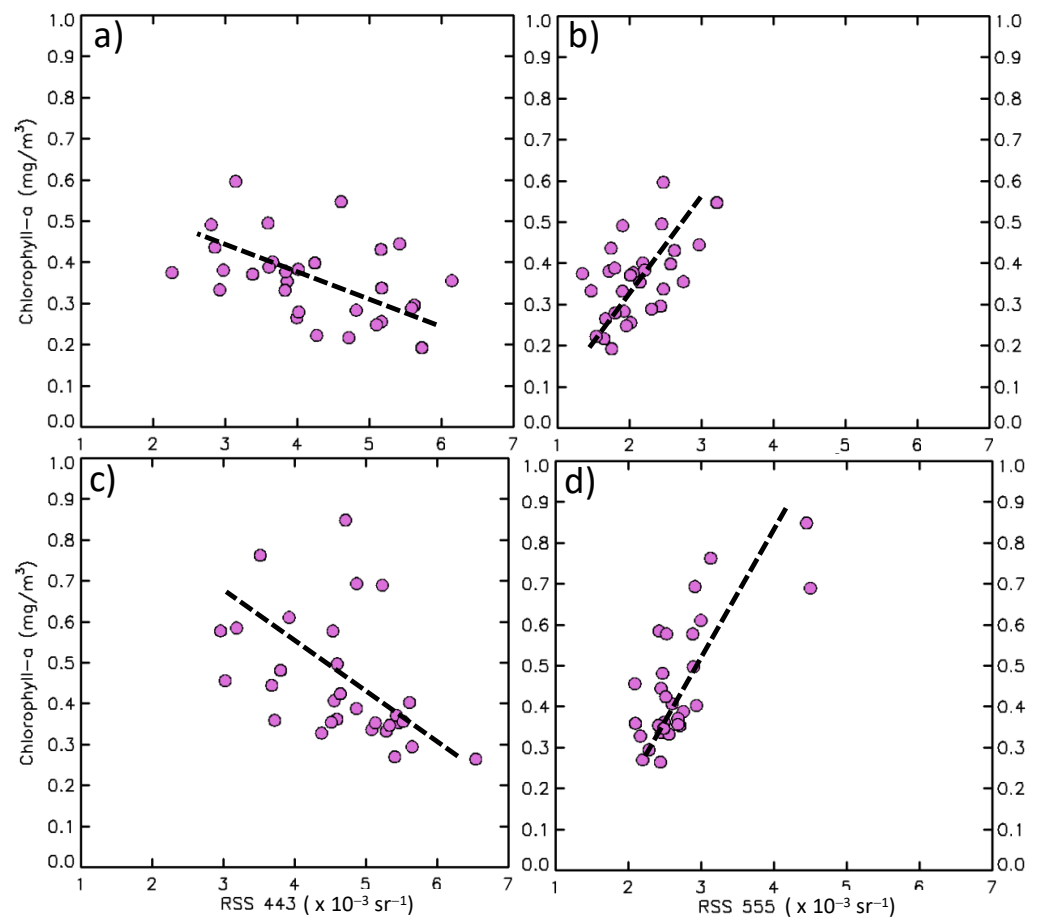


Figure 6. The scatter plots of monthly data of December, January, and February for (a) Rrs 443 vs. Chl-a and (b) Rrs 555 vs. Chl-a averaged from the first area in Figure 3a; (c) Rrs 443 vs. Chl-a and (d) Rrs 555 vs. Chl-a averaged from the second area in Figure 3a.

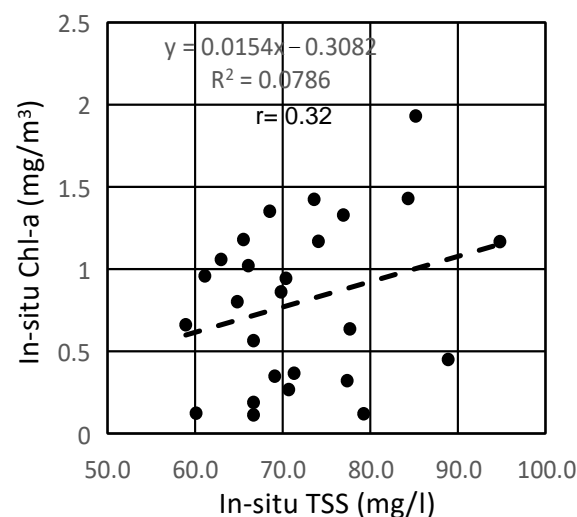


Figure 7. The scatter plot of in situ Chl-a and in situ TSS in the seas of Barrang Caddi Island (yellow dot in Figure 1c) on 8 September 2020. The value of r is for significant correlation analysis ($p < 0.05$).

4. Discussion

The previous study has shown that the southern coast of South Sulawesi is known as the high Chl-a area occurring during the boreal summer monsoon, which peaks in August [5,6]. In terms of magnitude, the highest Chl-a concentration at the second area on South

Sulawesi's western coast, which reaches 0.65 mg/m^3 , is lower than the southern coast, which reaches 1.4 mg/m^3 [5]. This may be related to the different generating mechanisms at the western and southern coasts of South Sulawesi. The strong upwelling at the southern coast of South Sulawesi may bring more nutrient-rich water than the river runoff due to the heavy rain. Nevertheless, the Chl-a concentration at the second area is higher than the other upwelling areas, such as in the Maluku Sea (e.g., [18,21,27]). This may correspond to the speed of wind-generated offshore; Ekman transport at the Maluku Sea is less than that at the southern coast of South Sulawesi. As a major path for monsoon wind, the wind speed along the southern coast of South Sulawesi is stronger than that at the Maluku Sea [28].

By conducting the climatological analysis, the present study enhances the seasonal variation of Chl-a along the western coast of South Sulawesi. Further, it is also important to investigate its inter-annual variation. As summarized by Wirasatriya et al. [25], the effect of El Niño Southern Oscillation on the magnitude of upwelling within the Indonesian Seas depends on the season. During summer or southeast monsoon season, El Niño (La Niña) tends to increase (decrease) upwelling intensity. Conversely, the intensity of northwest monsoon upwelling reduces (increases) during El Niño (La Niña). Furthermore, for the Chl-a variation in the coastal area, Siswanto et al. [4] showed that Chl-a concentration declines (increases) most notably during the concurrent positive Indian Ocean Dipole (IOD) and El Niño (negative IOD and La Niña) events. Since the area along the western coast of the South Sulawesi was not discussed in both previous studies, understanding the impact of the inter-annual climate variability to the Chl-a along the western coast of South Sulawesi will be beneficial for fisheries management in this area. This task is left for future study.

It is worth noting that the number of high Chl-a zones identified in Indonesian waters influenced by river runoff is still smaller than the upwelling areas. Wirasatriya et al. [25] have collected and identified upwelling locations in the Indonesian seas during the summer and rainy seasons. On the other hand, Siswanto et al. [4] found that, except for the coastal area of the northern Malacca Strait, the Chl-a variations at the coastal areas within the Indonesian seas are primarily influenced by the riverine nutrient fluxes and vary with the climatic events. As presented in the present study, the detailed feature of Chl-a blooms along the western coast of South Sulawesi during the rainy season is one example of how rainfall may influence Chl-a variation through the river runoff. This may trigger more investigation of other high Chl-a areas during the rainy season within the Indonesian Seas. However, careful interpretation of satellite-based Chl-a data should apply, as riverine organic/inorganic matter may bias the satellite Chl-a reading. Thus, collecting in situ data of Chl-a and suspended matter along the western coast of South Sulawesi and other coastal areas becomes the most valuable task to guarantee the accuracy of the satellite Chl-a reading. Further, it can be used to reproduce the new algorithm for the satellite-based Chl-a in those specified areas. This work is left for future study.

5. Conclusions

By taking advantage of blended products of satellite-based Chl-a data, we revealed the spatial and temporal variation of the Chl-a along the western coast of South Sulawesi. Two areas have been identified as high primary productivity areas occurring during the rainy season. The first and second areas are located at 119.0° E – 119.5° E ; 3.5° S – 4.0° S and 119.0° E – 119.5° E ; 4.6° S – 5.1° S , respectively. The monthly Chl-a variation in the first and second areas range from 0.35 mg/m^3 to 0.55 mg/m^3 and from 0.39 mg/m^3 to 0.6 mg/m^3 , respectively. The highest Chl-a concentration is observed in April and January for the first and second areas, respectively. The generating mechanism of the high Chl-a along the western coast of South Sulawesi is different from its southern coast, which is known as the coastal upwelling area. The existence of river runoff in these two areas may bring anthropogenic organic compounds during the peak of the rainy season, which increases the Chl-a concentration at the western coast of South Sulawesi.

Author Contributions: Conceptualization, A.W.; methodology, A.W. and A.D.P.; software, A.W.; formal analysis, A.W., K.K., F.R., A.R.J., and L.M.; investigation, A.W., K.K., and A.D.P.; resources, J.D.S., and L.M.; writing—original draft preparation, A.W. and K.K.; writing—review and editing, J.D.S., K.K., R.D.S., and I.I.; visualization, A.W., F.R., and A.D.P.; supervision, R.D.S. and I.I.; project administration, J.D.S. and A.R.J.; funding acquisition, A.W., J.D.S., and R.D.S. All authors have read and agreed to the published version of the manuscript.

Funding: This research is partially funded by non-APBN DPA LPPM 2021, Universitas Diponegoro Contract No: 329-121/UN7.6.1/PP/2021 and the Indonesian Endowment Fund for Education (LPDP) on behalf of the Indonesian Ministry of Education, Culture, Research and Technology managed by ITB under the Indonesia-MIT Program for Advanced Research and Technology (IMPACT). This project is also supported by the research scheme of Program Riset Unggulan COREMAP CTI 2021-2022 (17/A/DK/2021). Anindya Wirasatriya thanks the World Class Professor program managed by Indonesian Ministry of Education, Culture, Research and Technology. R. Dwi Susanto is supported by NASA grants #80NSSC18K0777 and NNX17AE79A through the University of Maryland, College Park.

Acknowledgments: OC-CCI Chl-a version 4.2 are available at <https://esa-oceancolour-cci.org/> (accessed on 28 March 2021), while MUR SST data can be downloaded at https://thredds.jpl.nasa.gov/thredds/catalog_ghrsst_gds2.html?dataset=MUR-JPL-L4-GLOB-v4.1 (accessed on 25 October 2021). ASCAT data is obtained from <http://marine.copernicus.eu/services-portfolio/access-to-products/> (accessed on 4 April 2021) while GSMAP data is from <https://sharaku.eorc.jaxa.jp/GSMaP/guide.html> (accessed on 10 April 2021).

Conflicts of Interest: The authors declare no conflict of interest. The funders had no role in the design of the study; in the collection, analyses, or interpretation of data; in the writing of the manuscript, or in the decision to publish the results.

References

- Welliken, M.A.; Melmambessy, E.H.P.; Merly, S.L.; Pangaribuan, R.D.; Lantang, B.; Hutabarat, J.; Wirasatriya, A. Variability Chlorophyll-a And Sea Surface Temperature As The Fishing Ground Basis Of Mackerel Fish In The Arafura Sea. In Proceedings of the 3rd International Conference on Energy, Environmental and Information System (ICENIS), Semarang, Indonesia 14–15 August 2018, 2018; Volume 73, pp. 4004. <https://doi.org/10.1051/e3sconf/20187304004>.
- Welliken, M.A.; Melmambessy, E.H.P.; Jumsar. Variability of Chlorophyll-a and Sea Surface Temperature, the effect on the Catches of Cakalang Fish in Sawu Sea of East Nusa Tenggara. *Int. J. Civil Eng. Tech.* **2019**, *10*, 715–723.
- Lahlali, H.; Wirasatriya, A.; Gensac, A.E.; Helmi, M.; Kunarso, Kismawardhani, R.A. Environmental aspects of tuna catches in the Indian Ocean, southern coast of Java, based on satellite measurements. In Proceedings of the 4th International Symposium on Geoinformatics 2018, Malang, Indonesia, 10–12 November 2018; pp. 1–6. <https://doi.org/10.1109/ISYG.2018.8612020>.
- Siswanto, E.; Horii, T.; Iskandar, I.; Gaol, J.L.; Setiawan, R.Y.; Susanto, R.D. Impacts of climate changes on the phytoplankton biomass of the Indonesian Maritime Continent. *J. Mar. Syst.* **2020**, *212*, 103451. <https://doi.org/10.1016/j.jmarsys.2020.103451>.
- Setiawan, R.Y.; Kawamura, H. Summertime Phytoplankton Bloom in the south Sulawesi Sea. *IEEE J. Sel. Topics Appl. Earth Observ. Rem. Sens.* **2011**, *4*, 241–244. <https://doi.org/10.1109/JSTARS.2010.2094604>.
- Utama, F.G.; Atmadipoera, A.S.; Purba, M.; Sudjono, E.H.; Zuraida, R. Analysis of upwelling event in Southern Makassar Strait. *IOP Conf. Ser. Earth Env. Sci.* **2017**, *54*, 12085. <https://doi.org/10.1088/1755-1315/54/1/012085>.
- Nurdin, S.; Mustapha, M.A.; Lihan, T. The relationship between sea surface temperature and chlorophyll-a concentration in fisheries aggregation area in the archipelagic waters of Spermonde using satellite images. *AIP Conf. Proc.* **2013**, *1571*, 466. <https://doi.org/10.1063/1.4858699>.
- Nurdin, S.; Mustapha, M.A.; Lihan, T.; Zainuddin, M. Applicability of remote sensing oceanographic data in the detection of potential fishing grounds of *Rastrelliger kanagurta* in the archipelagic waters of Spermonde, Indonesia. *Fish. Res.* **2017**, *196*, 1–12. <https://doi.org/10.1016/j.fishres.2017.07.029>.
- Sathyendranath, S.; Brewin, R.J.W.; Brockmann, C.; Brotas, V.; Calton, B.; Chuprin, A.; Cipollini, P.; Couto, A.B.; Dingle, J.; Doerffer, R.; et al. An ocean-colour time series for use in climate studies: The experience of the Ocean-Colour Climate Change Initiative (OC-CCI). *Sensors* **2019**, *19*, 4285. <https://doi.org/10.3390/s19194285>.
- Shi, W.; Wang, M. Observations of a Hurricane Katrina-induced phytoplankton bloom in the Gulf of Mexico. *Geophys. Res. Lett.* **2007**, *34*, L11607. <https://doi.org/10.1029/2007GL029724>.
- Zheng, G.M.; Tang, D.L. Offshore and nearshore chlorophyll increases induced by typhoon winds and subsequent terrestrial rainwater runoff. *Mar. Ecol. Prog. Ser.* **2007**, *333*, 61–74. <https://doi.org/10.3354/meps333061>.
- JPL MUR MEaSUREs Project. GHRSST Level 4 MUR Global Foundation Sea Surface Temperature Analysis. Ver. 4.1. PO.DAAC, CA, USA. 2015. Available online: <https://doi.org/10.5067/GHGM-4FJ04> (accessed on 2021-10-25).

13. Chao, Y.; Li, Z.; Farrara, J.D.; Hung, P. Blending sea surface temperatures from multiple satellites and in situ observations for coastal oceans. *J. Atmos. Oceanic. Technol.* **2009**, *26*, 1415–1426. <https://doi.org/10.1175/2009JTECHO592.1>.
14. Liu, Y.; Weisberg, R.H.; Law, J.; Huang, B. Evaluation of Satellite-Derived SST Products in Identifying the Rapid Temperature Drop on the West Florida Shelf Associated with Hurricane Irma. *Mar. Tech. Soc. J.* **2018**, *52*, 43–50. <https://doi.org/>.
15. Figa-Saldaña, J.; Wilson, J.J.W.; Attema, E.; Gelsthorpe, R.V.; Drinkwater, M.R.; Stoffelen, A. The Advanced Scatterometer (ASCAT) on the Meteorological Operational (MetOp) Platform: A Follow on for European Wind Scatterometers. *Canad. J. Rem. Sens.* **2002**, *28*, 404–412.
16. Otsuka, S.; Kotsuki, S.; Miyoshi, T. Nowcasting with data assimilation: A case of Global Satellite Mapping of Precipitation. *Weat. Forecast.* **2016**, *31*, 1409–1416.
17. Maslukah, L.; Setiawan, R.Y.; Nurdin, N.; Helmi, M.; Widiaratih, R. Phytoplankton Chlorophyll-a Biomass and the Relationship with Water Quality in Barrang Caddi, Spermonde, Indonesia. *Ecol. Eng. Env. Tech.* **2021**, in press.
18. Wirasatriya, A.; Setiawan, R.Y.; Subardjo, P. The effect of ENSO on the variability of chlorophyll-a and sea surface temperature in the Maluku Sea. *IEEE J. Sel. Topics Appl. Earth Observ. Rem. Sens.* **2017**, *10*, 5513–5518. <https://doi.org/10.1109/JSTARS.2017.2745207>.
19. Haack, T.; Burk, S.D.; Dorman, C.; Rogers, D. Supercritical flow interaction within the Cape Blanco–Cape Mendocino orographic complex. *Month. Weat. Rev.* **2001**, *129*, 688–708.
20. Shimada, T.; Sawada, M.; Sha, W.; Kawamura, H. Low-Level Easterly Winds Blowing through the Tsugaru Strait, Japan. Part I: Case Study and Statistical Characteristics Based on Observations. *Mont. Weat. Rev.* **2010**, *138*, 3806–3821.
21. Wirasatriya, A.; Sugianto, D.N.; Helmi, M.; Setiawan, R.Y.; Koch, M. Distinct Characteristics of SST Variabilities in the Sulawesi Sea and the Northern Part of the Maluku Sea During the Southeast Monsoon. *IEEE J. Sel. Topics Appl. Earth Observ. Rem. Sens.* **2019**, *12*, 1763–1770. <https://doi.org/10.1109/JSTARS.2019.2913739>.
22. Wirasatriya, A.; Setiawan, J.D.; Sugianto, D.N.; Rosyadi, I.A.; Haryadi, H.; Winarso, G.; Setiawan, R.Y.; Susanto, R.D. Ekman dynamics variability along the southern coast of Java revealed by satellite data. *Int. J. Rem. Sens.* **2020**, *41*, 8475–8496. <https://doi.org/10.1080/01431161.2020.1797215>.
23. Maslukah, L.; Zainuri, M.; Wirasatriya, A.; Salma, U. Spatial Distribution of Chlorophyll-a and Its Relationship with Dissolved Inorganic Phosphate Influenced by Rivers in the North Coast of Java. *J. Ecol. Eng.* **2019**, *20*, 18–25. <https://doi.org/10.12911/22998993/108700>.
24. Siswanto, E.; Tang, J.; Yamaguchi, H.; Ahn, Y.-H.; Ishizaka, J.; Yoo, S.; Kim, S.-W.; Kiyomoto, Y.; Yamada, K.; Chiang, C. et al. Empirical ocean-color algorithms to retrieve chlorophyll-a, total suspended matter, and colored dissolved organic matter absorption coefficient in the Yellow and East China Seas. *J. Oceanogr.* **2011**, *67*, 627–650. <https://doi.org/10.1007/s10872-011-0062-z>.
25. Wirasatriya, A.; Susanto, R.D.; Kunarso, K.; Jalil, A.R.; Ramdani, F.; Puryajati, A.D. Northwest monsoon upwelling within the Indonesian seas. *Int. J. Rem. Sens.* **2021**, *42*, 5437–5458. <https://doi.org/10.1080/01431161.2021.1918790>.
26. Maslukah, L.; Zainuri, M.; Wirasatriya, A.; Maisyarah, S. The Relationship among Dissolved Inorganic Phosphate, Particulate Inorganic Phosphate, and Chlorophyll-a in Different Seasons in the Coastal Seas of Semarang and Jepara. *J. Ecol. Eng.* **2020**, *21*, 135–142. <https://doi.org/10.12911/22998993/118287>.
27. Setiawan, R.Y.; Habibi, A. Satellite Detection of Summer Chlorophyll-a Bloom in the Gulf of Tomini. *IEEE J. Sel. Topics Appl. Earth Observ. Rem. Sens.* **2011**, *4*, 944–948. <https://doi.org/10.1109/JSTARS.2011.2163926>.
28. Setiawan, R.Y.; Habibi, A. SST cooling in the Indonesian seas. *Ilmu Kelaut. Indones. J. Mar. Sci.* **2010**, *15*, 42–46. <https://doi.org/10.14710/ik.ijms.15.1.42-46>.